

DESIGN AND TEST OF C-BAND COMPACT ACCELERATING STRUCTURE MADE OF LONGITUDINALLY-SPLIT TWO HALVES

Tetsuo Abe^{*,A)}, Masashi Kimura^{B)}, Nobuyuki Shigeoka^{B)}, Toshiyasu Higo^{A)}, Tomei Sugano^{B)}, Hiroshi Hara^{B)}, and Kyusaku Higa^{B)}

^{A)} High Energy Accelerator Research Organization (KEK)

^{B)} Mitsubishi Heavy Industries Machinery Systems, Ltd.

Abstract

Side-coupled structures operated with a $\pi/2$ mode have been widely used particularly for compact linacs. The structure has various advantages; however, there are some difficulties in fabrication due to many complicated parts to be bonded in the conventional fabrication method based on a mechanical unit of a disk. On the other hand, longitudinally-split structures are easy to fabricate due to a small number of parts, only two halves or four quadrants. In recent years, in collaboration between Mitsubishi Heavy Industries and KEK, we have been developing a longitudinally-split side-coupled C-band structure fabricated in two halves with a high shunt impedance based on successful experiences on the quadrant-type X-band CLIC prototype structure developed at KEK. We report the status, results and a plan of this project.

INTRODUCTION

RF accelerating tubes are often used for accelerating electrons (or positrons) over 1 MeV. Such tubes are mostly made of oxygen free copper, are fabricated by machining and stacking dozens of disks, and then bonding them by diffusion bonding or brazing (“disk-stacked type” shown in Fig. 1(a)). Although such disks can be made by turning so that very smooth surfaces with an average roughness (R_a) smaller than 100 nm can be achieved, the fabrication is cumbersome and complicated due to a large number of parts of disks. On the other hand, there is an “orthogonal” fabrication method: “longitudinally-split type”¹ as shown in Fig. 1(b), where accelerating structures are divided into two halves or four quadrants independent of the number of cells. Because halves or quadrants can be made by milling at once, and the fabrication is very easy, we can expect significant cost reduction in money and time [1], possibly leading to sustainability improvements. The longitudinally-split type has other advantages over the disk-stacked type:

- No surface current due to an accelerating mode flows across any bonding junction;
- Structures can be mechanically bonded far from accelerating fields.

However, the longitudinally-split type has some disadvantages, including

- Possibility of virtual leak between halves or adjacent quadrants,

* tetsuo.abe@kek.jp

¹ Both “longitudinally-split type” and “disk-stacked type” are coined by the authors.

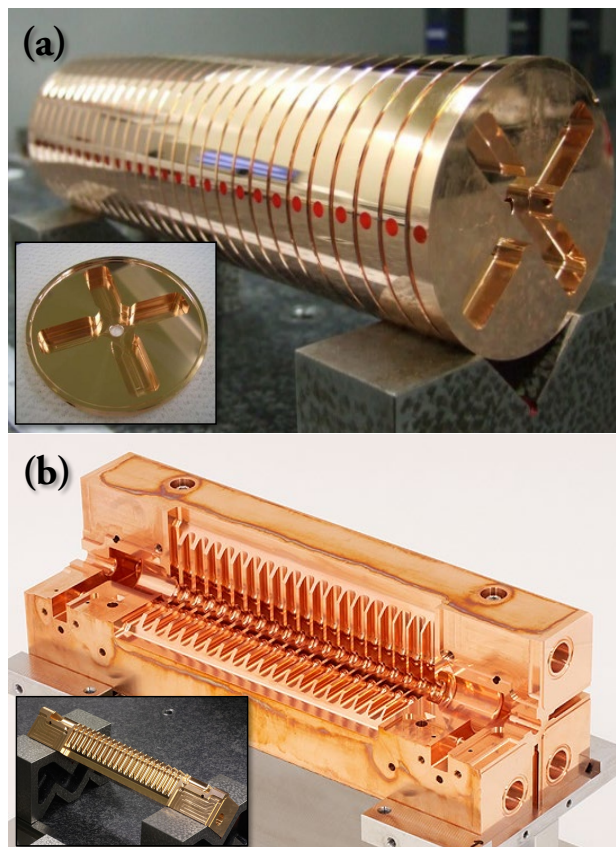


Figure 1: Two types of “orthogonal” accelerating structures: (a) disk-stacked type, and (b) longitudinally-split type.

- Field enhancements at the edge of halves or quadrants, and
- Difficulty in achieving a very smooth surface due to milling only, typically $R_a \geq 100$ nm.

We overcome the above top two disadvantages by improving the design [2], and demonstrated the high-field performance using a single-cell test cavity made of four quadrants based on the improved design, where the measured breakdown rate at a high accelerating gradient of 100 MV/m was low enough for the future linear collider of CLIC [3]. In addition, we established a fabrication method for a full-scale multi-cell accelerating tube based on the improved design [4] although we have not yet performed its high-field test due to the fire that occurred in our X-band high-field test facility (Nextef) in 2019.

After the authors demonstrated in 2017 that the improved longitudinally-split structure can provide a good high-field

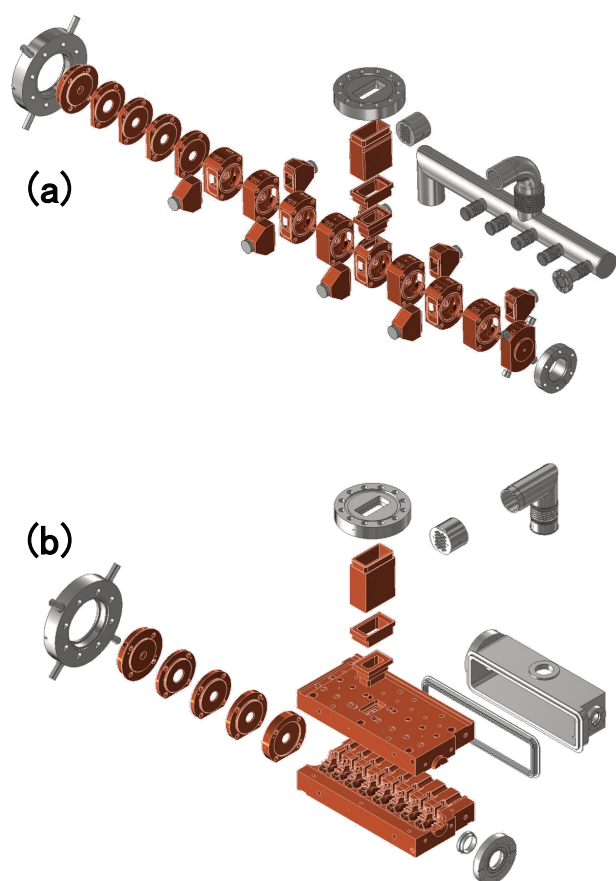


Figure 2: Exploded diagrams of the (a) conventional disk-stacked type and (b) new longitudinally-split type structures.

performance, various such structures appeared in various practical and experimental accelerators or test facilities, including an alternative design of an X-band high-gradient accelerating structure for the CLIC main linac [5], a C-band distributed coupling structure for Cool Copper Collider: C³ [6], and a compact X-band RF photogun made from two halves [7]. In this paper, the authors show results of application of the improved longitudinally split type to a C-band compact medical linac which has a side-coupled structure operated in a stable standing-wave $\pi/2$ mode. Because the linac has been fabricated so far as a disk-stacked type, so that it is difficult to fabricate it due to its complexity. The authors expect to demonstrate the effectiveness of the improved longitudinally-split type fabrication method through this development.

NEW DESIGN FEATURES

The accelerating structure consists of two sections for bunching and main acceleration, both of which are filled with electromagnetically-coupled $\pi/2$ modes excited by 5.7 GHz RF power injection through a single waveguide port. The buncher section has an alternating periodic structure (APS), and is not complicated, so that we do not change the design of the buncher section. On the other hand, we have changed

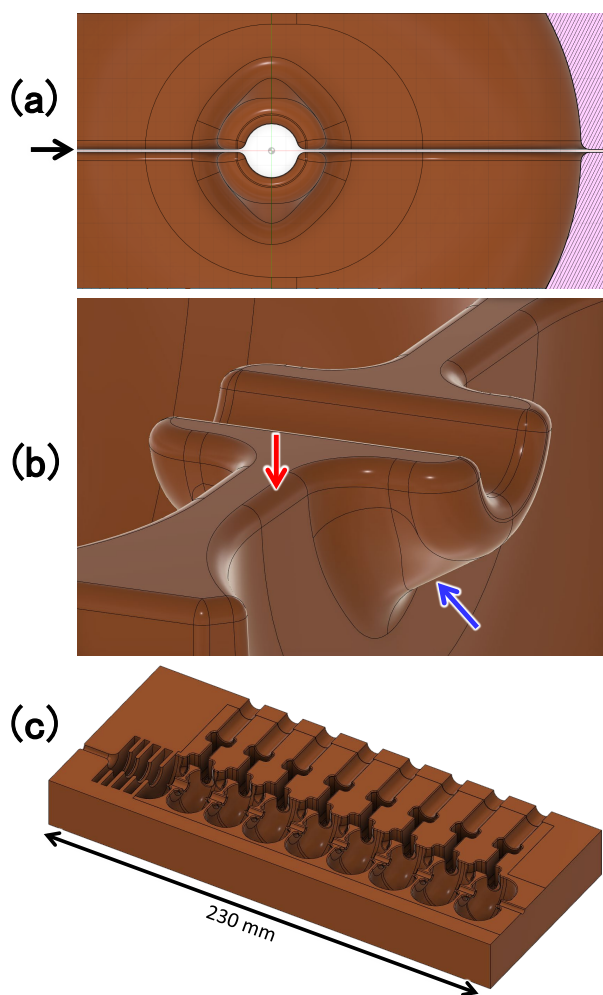


Figure 3: New design features. (a) 0.2 mm small gap between the two halves indicated with a black arrow. (b) R0.6mm large round chamber indicated with a red arrow, and “skirt” shape indicated with a blue arrow. (c) All the coupling cavities located to one side.

the design of the section for main acceleration with a side-coupled structure as shown in Fig. 2. The number of parts to be bonded is 59 for the conventional structure shown in Fig. 2(a), that is largely reduced to 25 for the new structure shown in Fig. 2(b), allowing reduction in the number of brazing from 2 to 1, i.e, the 59 parts in Fig. 2(a) are bonded into one through two step brazing, on the other hand, the 25 parts in Fig. 2(b) can be bonded into one through a single brazing.

The significant features of the new design are:

- Small gap of 0.2 mm shown in Fig. 3(a) indicated with a black arrow in order to remove the possibility of virtual leaks between the two halves,
- Large round chamfer of R0.6mm in order to suppress field enhancements,
- Nose cones with a long protuberance, shown in Fig. 3(b), for a high shunt impedance,

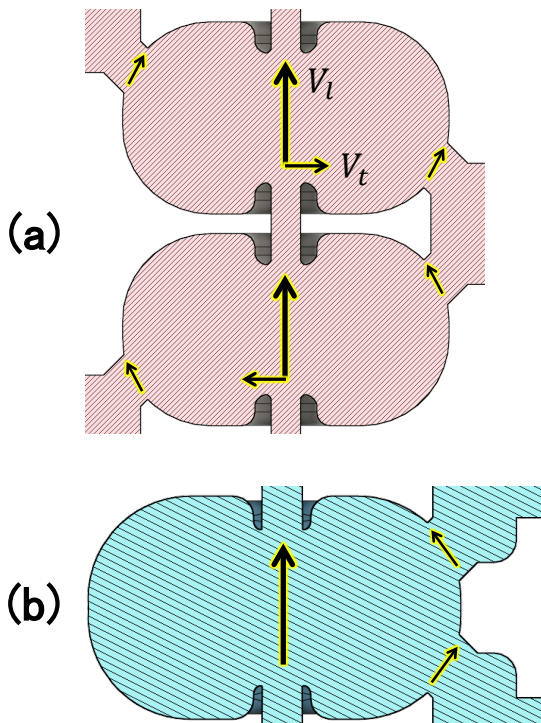


Figure 4: Schematic diagram of the accelerating electric field. In the case of the (a) conventional and (b) new design. V_l (V_t) indicates the longitudinal (transverse) component of the accelerating voltage.

- “Skirt” shape at the nose cone for effective machining so that final machining is easily possible with a single milling tool, where the shunt-impedance deterioration due to the skirt is smaller than 0.1%, and
- All the coupling cavities located to one side for material saving.

Since all the coupling cavities are located to one side, transverse kicks by the accelerating mode are unavoidable. Therefore, we modified the cross-sectional shape of the accelerating cell from circle to racetrack with the beam axis having an offset with respect to the central axis of the accelerating cell so that the amplitude of the longitudinal component of the accelerating electric field has a symmetric distribution in the transverse plane with respect to the beam axis. On the other hand, its phase cannot be symmetric with respect to the beam axis in the transverse plane. we calculated the deflection of the accelerating voltage vector due to the asymmetry according to the Panofsky-Wenzel theorem [8], and found it to be very small, $V_t/V_l \approx 20 \mu\text{rad}$, where V_t (V_l) indicates a transverse (longitudinal) accelerating voltage. This deflection is negligible for compact linacs with a length short than 1 m even if the deflection is in the same direction for all the accelerating cells. Even with the above modification, the accelerating electric field has a non-zero transverse component due to the broken symmetry in the geometry. Figure 4(a) shows a significant transverse voltage due to the two apertures to the coupling cavities located di-

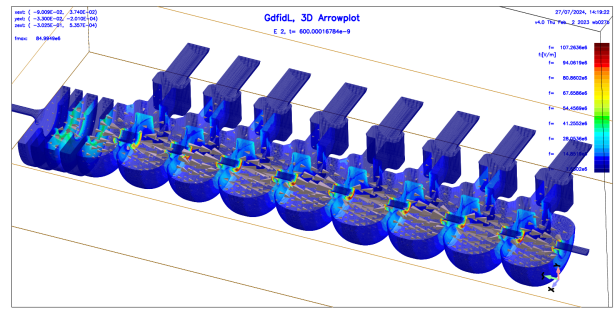


Figure 5: Electric field of the accelerating $\pi/2$ mode for the final design of the first full-scale prototype.

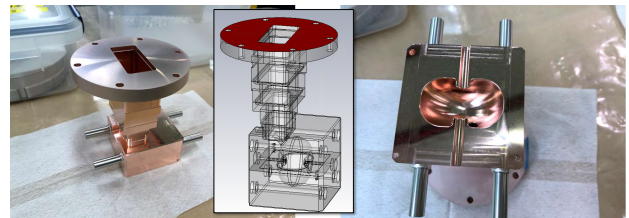


Figure 6: Single-cell test cavity for high field testing.

agonally in the conventional design, where the deflection in an accelerating cell is calculated to be $V_t/V_l \approx 20 \text{ mrad}$. The sign of the deflection is reversed in the neighboring accelerating cell, so that accelerated electrons undulate through the accelerating cells for the conventional design. On the other hand, as shown in Fig. 4(b), such transverse component is mostly canceled within an accelerating cell in the new design, resulting in a tiny transverse component in the accelerating field. Figure 5 shows an electric field of the accelerating $\pi/2$ mode for the final design of the first full-scale prototype, simulated with GdfidL [9]. A small field is excited in the coupling cavities due to the existence of the buncher section.

Our accelerating structure has a high shunt impedance of approximately $140 \text{ M}\Omega/\text{m}$ at 5.7 GHz in the relativistic section, corresponding to approximately $180 \text{ M}\Omega/\text{m}$ at 9.3 GHz, which is significantly higher than that of the longitudinally-split type of a side-coupled structure in the earlier development: $124.3 \text{ M}\Omega/\text{m}$ in the relativistic section [10].

HIGH-FIELD TEST

To demonstrate the high-field performance of the new design, we fabricated a single-cell test cavity as shown in Fig. 6. The inner surface has an average roughness of $R_a \approx 0.6 \mu\text{m}$, that is smaller than the skin depth of copper at 5.7 GHz of $\approx 0.9 \mu\text{m}$. The measured unloaded quality factor is 99.9% of the simulated one. The achieved profile accuracy is $\approx 20 \mu\text{m}$.

We used a C-band klystron for this high-field test, whose maximum output RF power is 150 kW. The available RF pulse width is $4 \mu\text{s}$ at maximum, which is the same as in the specification of the relativistic section of this compact linac. With the 150 kW output RF power, an accelerating

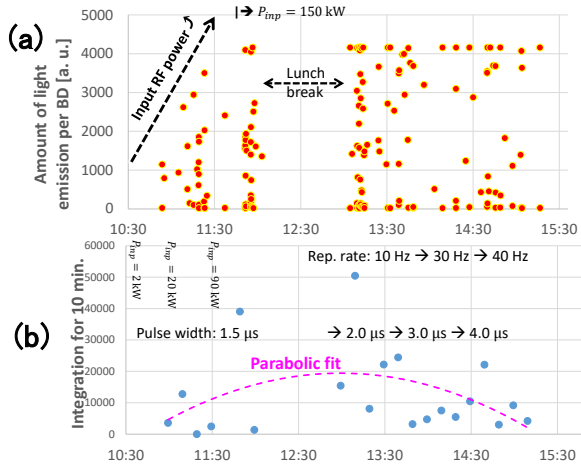


Figure 7: One-day history of the high-field test. (a) Amount of light emission per breakdown detected with the on-axis video camera. (b) Average for ten minutes of the amount of light emission in (a).

gradient of 27 MV/m can be excited, which is close to one in the specification for the relativistic section ($\approx 30 \text{ MV/m}$).

To detect vacuum breakdowns in the test cavity during high-field testing, we put a video camera on-axis, allowing us to observe light emissions through the beam port of the test cavity when breakdown occurred. Figure 7(a) shows the amount of light emission for each breakdown as a function of time. Before 11:30 AM, we increased the RF power up to the maximum of 150 kW. After the lunch break, we increased the repetition rate from 10 Hz to 40 Hz, and enlarged the RF pulse width from 1.5 μm to 4 μm. Figure 7(b) shows the average amount of light emission for ten minutes, that shows no obvious rising even though with the higher repetition rates and longer RF pulse widths, which means a good conditioning effect obtained in a single day only. The final breakdown rate is approximately once per ten minutes, that is $\approx 4 \times 10^{-5}$ /pulse/cell at an accelerating gradient of 27 MV/m with an RF pulse width of 4 μm. It should be noted that the breakdown rate should further decrease if we had continued the high-field test which was terminated due to the time limitation.

FULL-SCALE PROTOTYPE

Since we demonstrated the high-field performance of the new design using the single-cell test cavity, we fabricated a full-scale prototype and performed low-power RF measurements [11]. Surprisingly, we found that the electric-field distribution on the beam axis measured with the bead-pull method was in very good agreement with the design even before frequency tuning as shown in Fig. 8(a), that was not seen in the measurement for the conventional disk-stacked type as shown in Fig. 8(b). The same trend was seen in the past development of the X-band CLIC prototype structures (traveling-wave) with a waveguide damping as shown in Fig. 9 which shows measurements of the on-axis accelerating

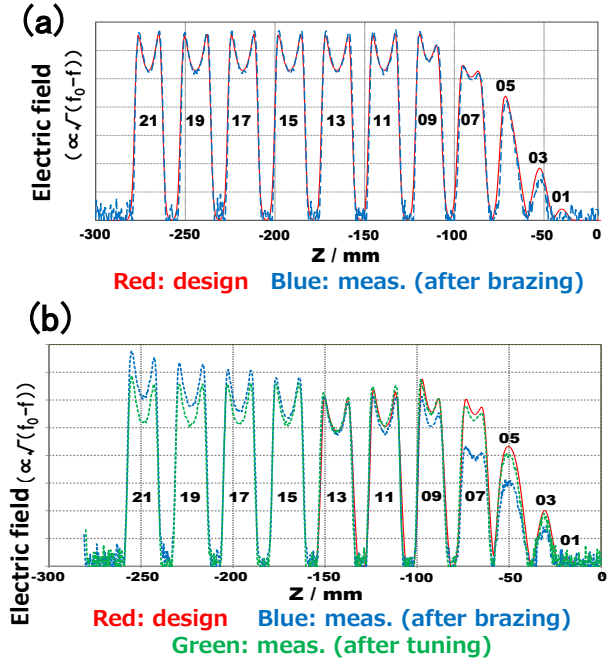


Figure 8: Electric-field distribution on the beam axis measured with the bead-pull method before frequency tuning (except for the green one in (b)) for (a) this accelerating structure with the new design, and (b) the conventional disk-stacked type structure.

field distribution before frequency tuning. Although large standing-wave components are seen in the measurements for the disk-stacked type structures as shown in Fig. 9(b) and (c), only small standing-wave components can be seen in that for the improved longitudinally-split type structure with almost the same design on the cells, as shown in Fig. 9(a). The difference in the agreement or disagreement of the on-axis accelerating field can be attributed to the difference in the number of parts to be bonded, that is one of the significant features of the improved longitudinally-split type.

The details on the fabrication of the full-scale prototype and low-power RF measurements are found in [11].

SUMMARY AND FUTURE PLANS

We established the new fabrication method for accelerating tubes of the improved longitudinally-split type at X-band, including the demonstration of the high-field performance and fabrication of the full-scale prototype. In this development, we are applying the new fabrication method to the C-band compact linac with the side-coupled structure and a high shunt impedance. We have demonstrated the high-field performance of the new design using the single-cell test cavity of the accelerating cell. Through fabrication and testing of a five-cell test structure, we have fabricated a full-scale prototype this year. We will finish its frequency tuning soon, and have a plan to perform a beam test in order to measure various quantities including radiation doses due to

REFERENCES

- [1] T. Abe, Y. Higashi, Y. Arakida, T. Higo, S. Matsumoto, T. Shidara, and T. Takatomi, "Quadrant-Type X-Band Single-Cell Structure for High Gradient Tests," in *Proceedings of the 9th Annual Meeting of Particle Accelerator Society of Japan, THPS095*, August 2012. https://www.pasj.jp/web_publish/pasj9/proceedings/PDF/THPS/THPS095.pdf
- [2] T. Abe, Y. Ajima, Y. Arakida, T. Higo, H. Inoue, N. Kudo, S. Matsumoto, and T. Takatomi, "Fabrication of Quadrant-Type X-Band Single-Cell Structure Used for High Gradient Tests," in *Proceedings of the 11th Annual Meeting of Particle Accelerator Society of Japan, SUP042*, August 2014. https://www.pasj.jp/web_publish/pasj2014/proceedings/PDF/SUP0/SUP042.pdf
- [3] T. Abe, T. Takatomi, T. Higo, S. Matsumoto, and Y. Arakida, "High-Gradient Test Results on a Quadrant-Type X-Band Single-Cell Structure," in *Proceedings of the 14th Annual Meeting of Particle Accelerator Society of Japan, WEP039*, August 2017. https://www.pasj.jp/web_publish/pasj2017/proceedings/PDF/WEP0/WEP039.pdf
- [4] T. Abe, T. Takatomi, Y. Higashi, T. Higo, and S. Matsumoto, "Fabrication of Improved Quadrant-Type X-Band High-Gradient Accelerating Structures," in *Proceedings of the 16th Annual Meeting of Particle Accelerator Society of Japan, WEOH04*, August 2019. https://www.pasj.jp/web_publish/pasj2019/proceedings/PDF/WEOH/WEOH04.pdf
- [5] T. Argyropoulos *et al.*, "Design, fabrication, and high-gradient testing of an X-band, traveling-wave accelerating structure milled from copper halves," *Phys. Rev. Accel. Beams*, vol. 21, no. 6, p. 061001, 2018. <https://journals.aps.org/prab/abstract/10.1103/PhysRevAccelBeams.21.061001>
- [6] <https://web.slac.stanford.edu/c3/>
- [7] T. Lucas, X. Stragier, P. Mutsaers, and O. Luiten, "RF design of a compact, X-band travelling-wave RF photogun made from halves," *Nuclear Instruments and Methods in Physics Research Section A: Accelerators, Spectrometers, Detectors and Associated Equipment*, vol. 1013, p. 165651, 2021. <https://www.sciencedirect.com/science/article/pii/S0168900221006367>
- [8] W. K. H. Panofsky and W. Wenzel, "Some Considerations Concerning the Transverse Deflection of Charged Particles in Radiofrequency Fields," *Rev. Sci. Instrum.*, vol. 27, p. 967, 1956.
- [9] <http://www.gdfidl.de/>
- [10] S. V. Kutsaeva, R. Agustsson, R. Berrya, S. Bouchera, and A. Y. Smirnova, "Electron Accelerator for Replacement of Radioactive Sources in Insect Sterilization Facilities," *Phys. Atom. Nuclei*, vol. 84, p. 1743, 2021. <https://doi.org/10.1134/S1063778821100215>
- [11] M. Kimura, T. Sugano, N. Shigeoka, H. Hara, K. Higa, T. Abe, and T. Higo, "Fabrication of C-band Compact Accelerating Structure made of Longitudinally-Split Two Halves," in *these proceedings, FRP042*, August 2024.

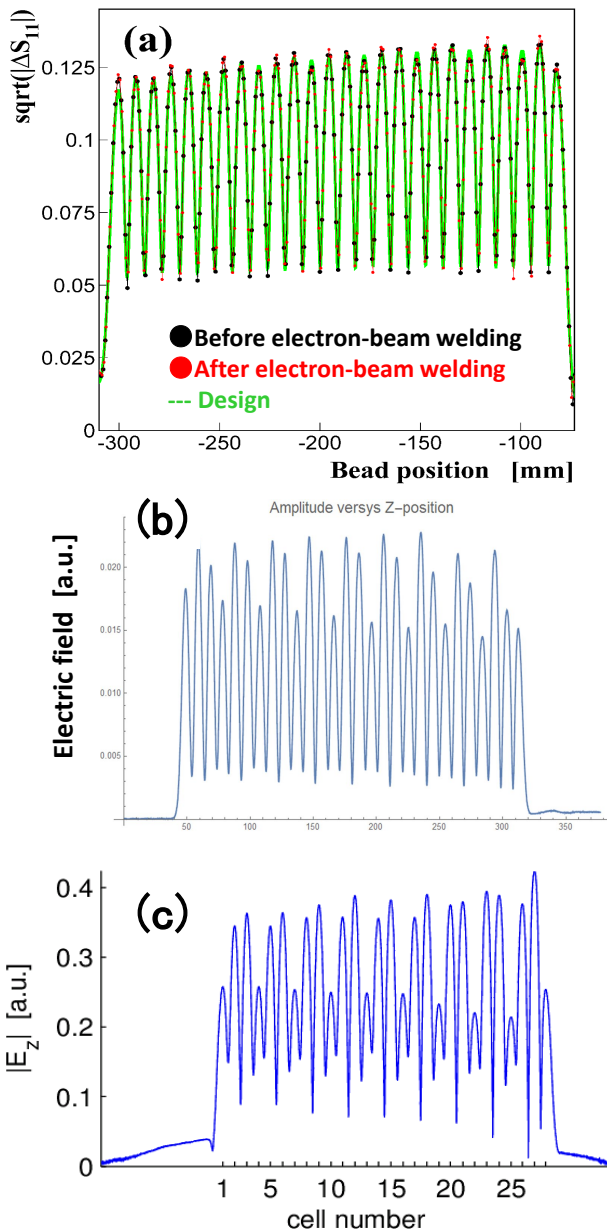


Figure 9: Electric-field distribution on the beam axis measured with the bead-pull method before frequency tuning for X-band waveguide-damped full-scale traveling-wave accelerating tubes fabricated in (a) four quadrants (improved longitudinally-split type) [4], and conventional disk-stacked type structures fabricated by (b) KEK and (c) CERN.

and transmission percentage of accelerated beams, resulting in a feedback to improvements for the second full-scale prototype.

ACKNOWLEDGEMENTS

We are grateful to Prof. Mitsuhiro Yoshida for allowing us to perform the high-field test at his C-band high-power test stand.